Nanocarbon-intercalated and Fe-N-codoped Graphene as a Highly Active Noble-metal-free Bifunctional Electrocatalyst for Oxygen Reduction and Evolution

Daping He,[abc] *Yuli Xiong,*[c] *Jinlong Yang,*[a] *Xu Chen,*[a] *Zhaoxiang Deng,*[b]* *Mu Pan,*[a] *Yadong Li*[bd] *and Shichun Mu*[a]*

[a.] State Key Laboratory of Advanced Technology for Materials Synthesis and Processing, Wuhan University of Technology, Wuhan 430070 (China).

[b.] Center of Advanced Nanocatalysis (CAN-USTC), University of Science and Technology of China, Hefei 230002 (China).

[c.] Department of Chemistry, University of Bath, Bath, Somerset BA2 7AY (UK)

[d.] Department of Chemistry, Tsinghua University, Beijing 100084 (China).

*Corresponding authors: zhxdeng@ustc.edu.cn; msc@whut.edu.cn.

Catalyst synthesis

Chemicals. Graphite powder was purchased from Sigma Aldrich. Carbon nanosphere (Vulcan XC-72) was a product from Cabot Corporation. Commercial Pt/C (20 wt. %) catalysts and Nafion (5 wt.%) were purchased from Johnson Mattey and Dupont, respectively. All chemicals were of analytical grade, and used without further purification.

Preparation of graphene oxide (GO). GO was synthesized with the graphite powder as a starting material, following a modified Hummer's method described previously.[1]

Preparation of Fe-N-CIG. Fe-N-CIG was synthesized via a lyophilization-assisted process. 0.1 g GO and 1 g urea were dispersed in 100 mL of deionized water. To the above solution were added 0.02 g carbon nanospheres (CNS, Vulcan XC-72) and 1 mL of ferric ammonium sulfate solution (0.5 mg mL^{-1} in terms of iron), followed by an ultrasonication for 30 min. The above mixture was continuously stirred for 2 hours, and the solid product was collected by rotary evaporation. The resulting product was then lyophilized and transferred to a quartz boat for a subsequent thermal treatment at 900 ºC in a tube furnace for 30 min in an argon flow. After cooling down to room temperature under Ar protection, the Fe-N-CIG material was obtained.

Preparation of Fe-N-G, N-CIG, N-G and Fe-N-CNS hybrids. The Fe-N-G, N-CIG, and N-G hybrids were synthesized via similar procedures as for the Fe-N-CIG catalyst but in the absence of CNS, iron reagent, or both. Fe-N-CNS corresponded to a product in the absence GO, with a 1:10 mass ratio between CNS (Vulcan XC-72) particles and urea.

Characterizations. N_2 adsorption/desorption isotherms were obtained at 77 K with a Micromeritics ASAP 2020 Brunauer-Emmett-Teller (BET) analyzer. X-ray photoelectron spectroscopy (XPS) measurements were carried out on a VG Scientific ESCALAB 210 electron spectrometer using Mg K_α radiation under a vacuum of 2×10^{-8} Pa. Morphologies of as-prepared catalysts were checked with a JEOL JEM6700 scanning electron microscope (SEM) operated at 10 kV and a JEOL 2010 transmission electron microscope (TEM).

Electrochemical measurements

General information

Electrochemical measurements were conducted at room temperature with a three-electrode system controlled by a CHI760E electrochemical work station (Chenhua Inc., Shanghai, China). A Pine AFMSRCE electrode rotator was used for rotating disk electrode (RDE) experiments. A silver/silver chloride (3 M KCl) electrode was used as a reference electrode, and a platinum wire was used as a counter electrode. The electrolyte was a 0.1 M KOH aqueous solution. Prior to each measurement, the electrolyte was bubbled with oxygen or nitrogen until saturation. A constant O_2 or N_2 flow was then maintained in the headspace of the electrolyte during the whole experiment. Electrochemical impedance spectroscopy (EIS) was measured at room temperature with the same cell configuration at an open circuit potential perturbed with a 5 mV amplitude sinusoidal voltage ranging from 1 MHz to 1 Hz.

Cyclic voltammetry (CV) on a static electrode

5 mg of as-prepared catalyst and 100 μL of 5 wt. % Nafion solution were mixed with 1 mL of isopropanol, followed by a sonication for at least 15 min to form a homogeneous catalyst ink. 10μL of the ink was loaded onto a glassy carbon (GC) disk electrode with a diameter of 5 mm, corresponding to a catalyst loading of ~0.23 mg cm^{-2}. The catalyst layer

was allowed to dry under ambient conditions before a CV measurement. The catalyst-loaded GC working electrode was cycled within specified potential window at least 3 times before a data collection at a scan rate of 10 mV s^{-1}.

Rotating disk electrode (RDE) voltammetry

To obtain steady state voltammetric data on an RDE, the catalyst ink was loaded on a glassy carbon RDE (5 mm diameter), which was then mounted on an electrode rotator. The polarizing potential of the catalyst-loaded RDE working electrode was scanned linearly and cathodically at a rate of 5 mV s^{-1} with an electrode rotation speed ranging between 400 and 1600 rpm. Koutecky-Levich plots (J^{-1} vs. $\omega^{-1/2}$) at various electrode potentials were employed to extract the number (*n*) of transferred electrons from the slopes of the fitting lines based on the Koutecky-Levich equation:[2, 3]

$$\frac{1}{J}=\frac{1}{J_L}+\frac{1}{J_K}=\frac{1}{B\,\omega^{1/2}}+\frac{1}{J_K}$$

$$B=0.62nFC_O(D_O)^{2/3}v^{-1/6}$$

where J is the experimentally measured current density, J_L is the diffusion-limiting current density, J_K is the kinetic current density, ω is the angular velocity, n is the number of transferred electrons, F is the Faraday constant, C_O is the bulk concentration of O_2 (1.26×10^{-3} mol L^{-1}), D_O is the diffusion coefficient of O_2 (1.9×10^{-5} cm^2 s^{-1}), and v is the kinematic viscosity of the electrolyte (1.09×10^{-2} cm^2 s^{-1}). [4] The value of n is calculated from the slope of the Koutecky-Levich plot. A further calibration of n can be done according to the standard Pt/C catalyst (4e transfer) as it is not realistic to have an n greater than 4.

Rotating ring-disk electrode (RRDE) measurement

12μL of the catalyst ink was loaded on the glassy carbon disk with a diameter of 5.6 mm (corresponding to a catalyst loading of ~0.22 mg cm^{-2}) of an RRDE. The potential of the catalyst-modified disk electrode was scanned linearly and cathodically at a rate of 5 mV s^{-1}. The platinum ring electrode of the RRDE was maintained at a constant oxidizing potential of 1.5 V vs. RHE. Based on the RRDE data, the percentage of HO_2^- by-products and electron transfer numbers (n) were calculated from the following equations:[3, 5]

$$\%HO_2^-=\frac{200I_r/N}{I_d+I_r/N}$$

$$n = \frac{4I_d}{I_d + I_r/N}$$

where I_d represents the disk current, $I_r$is the ring current, and N is the collection efficiency of the Pt ring electrode (determined to be 0.36 based on the reduction of $K_3Fe[CN]_6$).

RHE calibration

In the above electrochemical measurements, an Ag/AgCl (3 M KCl) electrode was employed as a reference electrode. The potential of the working electrode versus Ag/AgCl was then calibrated with respect to a reversible hydrogen electrode (RHE). The calibration was carried out in a high purity hydrogen saturated 0.1 M KOH by a CV test at a scan rate of 1 mV s^{-1}, with a Pt wire working electrode. As shown below, the thermo dynamic potential for the hydrogen electrode was taken to be the average of the two potentials at which the current crossed zero.[2] Based on this figure, we obtained E (vs. RHE) = E (vs. Ag/AgCl) + 0.97 V in 0.1 M KOH.

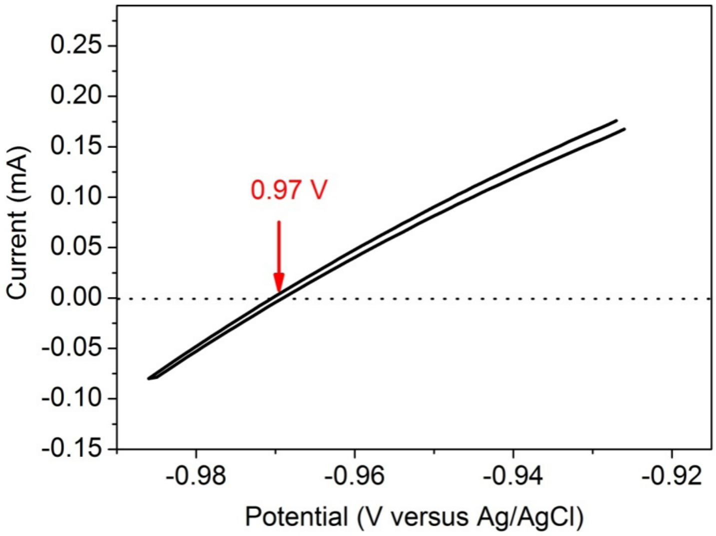

References

(1) W. S. Hummers, R. E. Offeman, *J. Am. Chem. Soc*. 1958, *80*, 1339.

(2) B. Lim, M. Jiang, P. H. C. Camargo, E. C. Cho, J. Tao, X. Lu, Y. Zhu, Y. Xia, *Science* 2009, *324*, 1302.

(3) Y. Liang, Y. Li, H. Wang, J. Zhou, J. Wang, T. Regier, H. Dai, *Nat. Mater*. 2011, *10*, 780.

(4) X. Q. Min, Y. H. Chen, M. W. Kanan, *Phys. Chem. Chem. Phys*. 2014, *16*, 13601.

(5) Z. S. Wu, S. Yang, Y. Sun, K. Parvez, X. Feng, K. Müllen, *J. Am. Chem. Soc*. 2012, *134*, 9082.

Supporting Figures

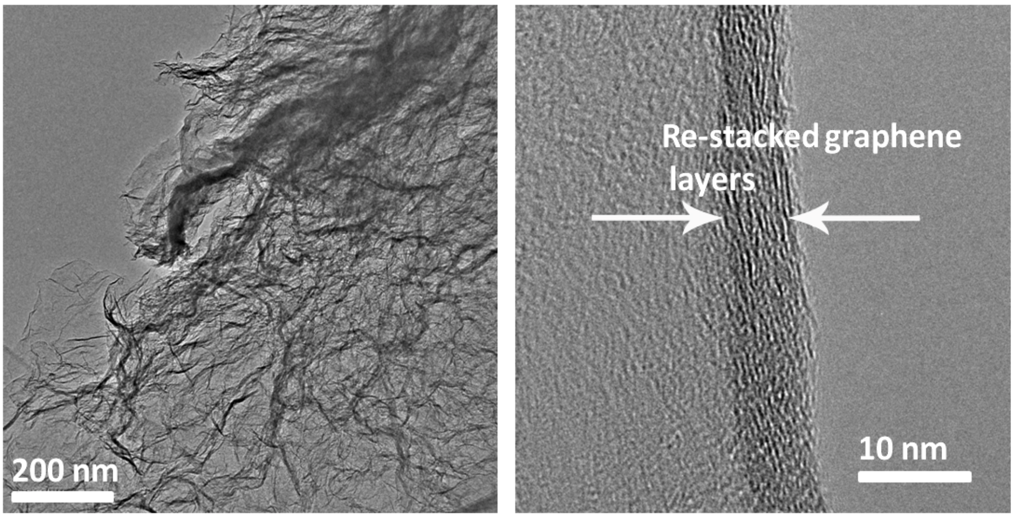

Figure S1. TEM images of the Fe-N-G catalyst under low (a) and high (b) magnifications.

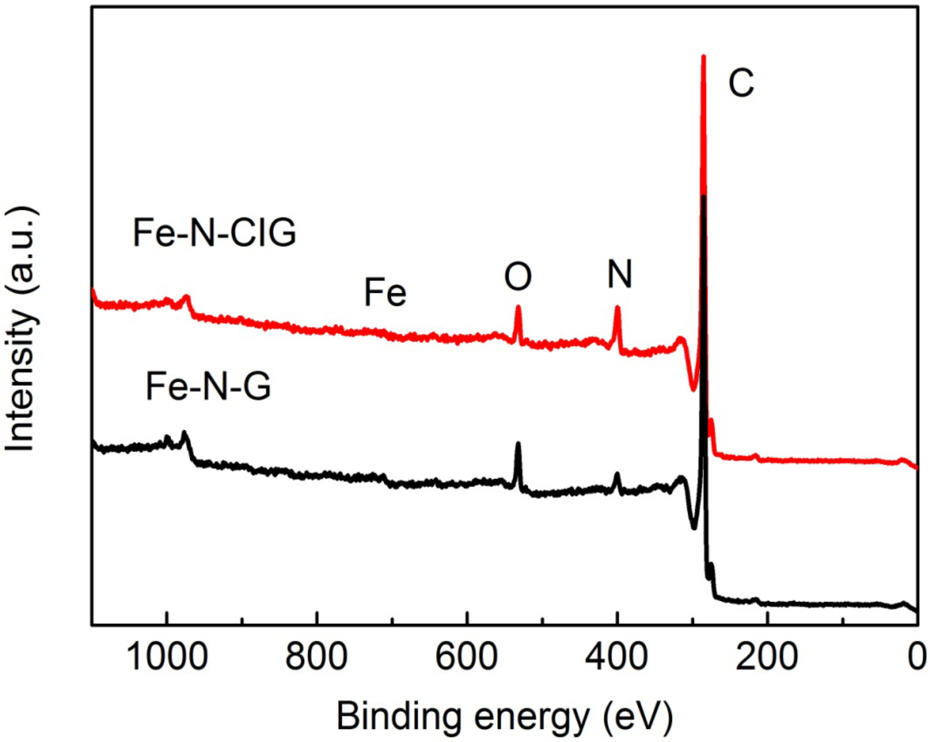

Figure S2. XPS survey spectra for the Fe-N-CIG and Fe-N-G catalysts.

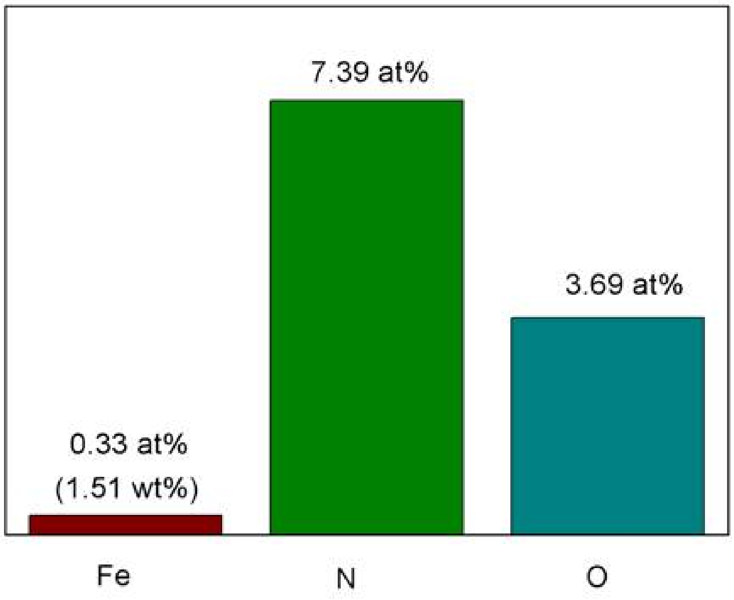

Figure S3. Atomic contents of iron, nitrogen, and oxygen in the Fe-N-CIG hybrid measured by XPS. The iron mass content was analysed by ICP-MS.

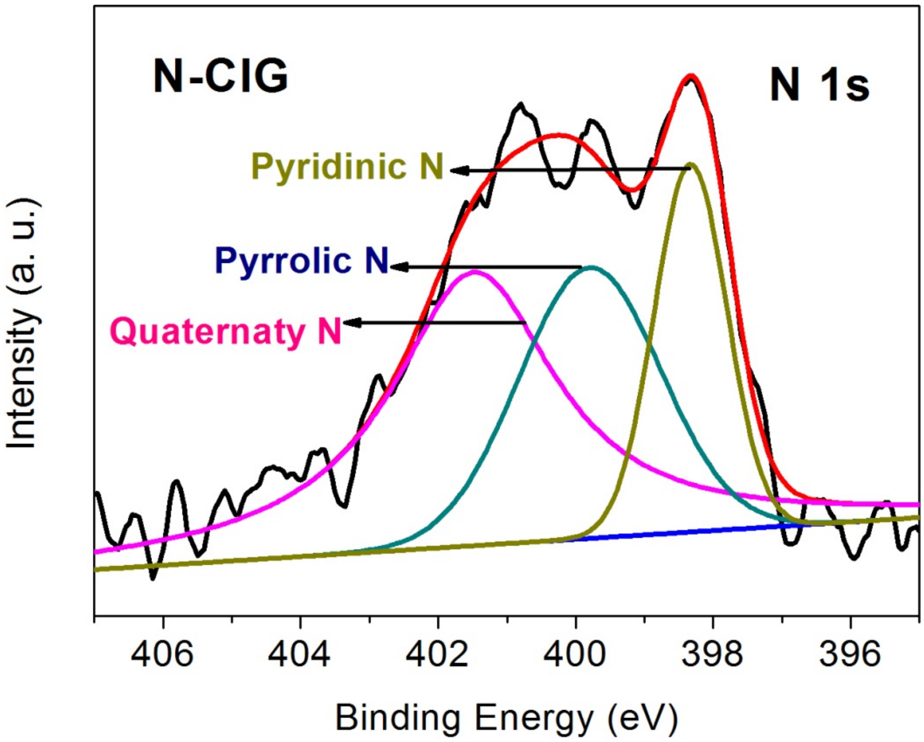

Figure S4. XPS spectrum of N 1s for the N-CIG catalyst.

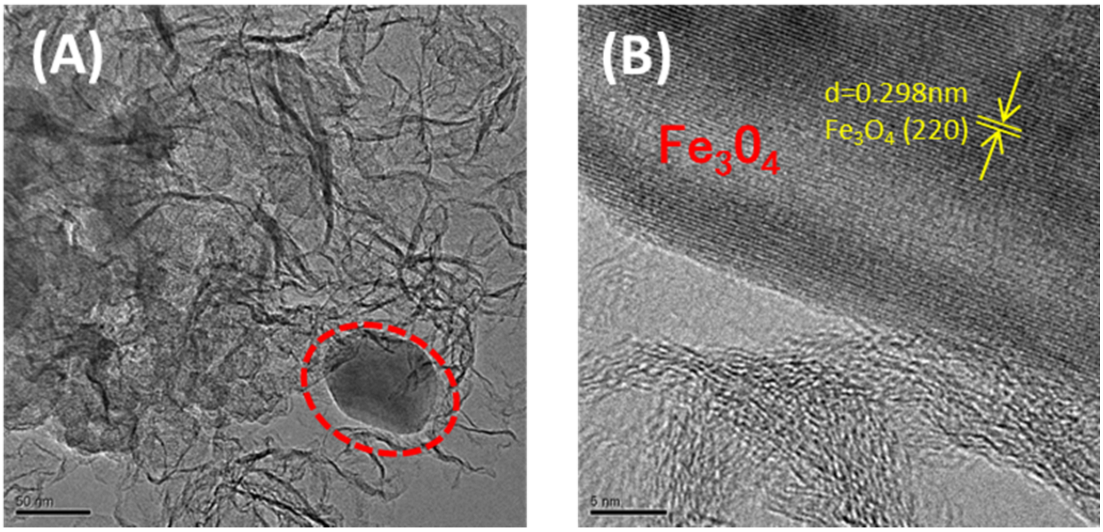

Figure S5 TEM images showing the existence of Fe_3O_4 nanoparticles in the Fe-N-CIG sample.

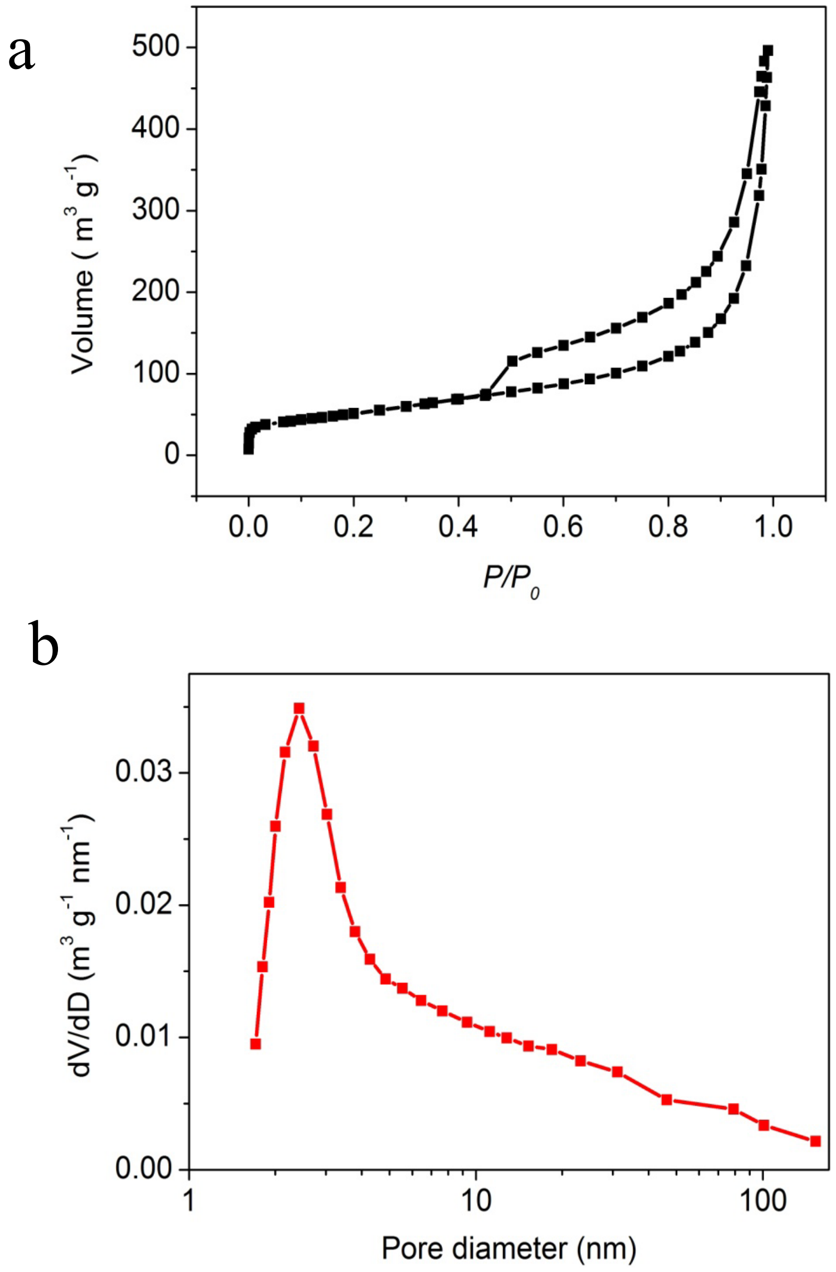

Figure S6. Nitrogen adsorption-desorption isotherm (a) and corresponding pore size distribution (b) of the Fe-N-G catalyst.

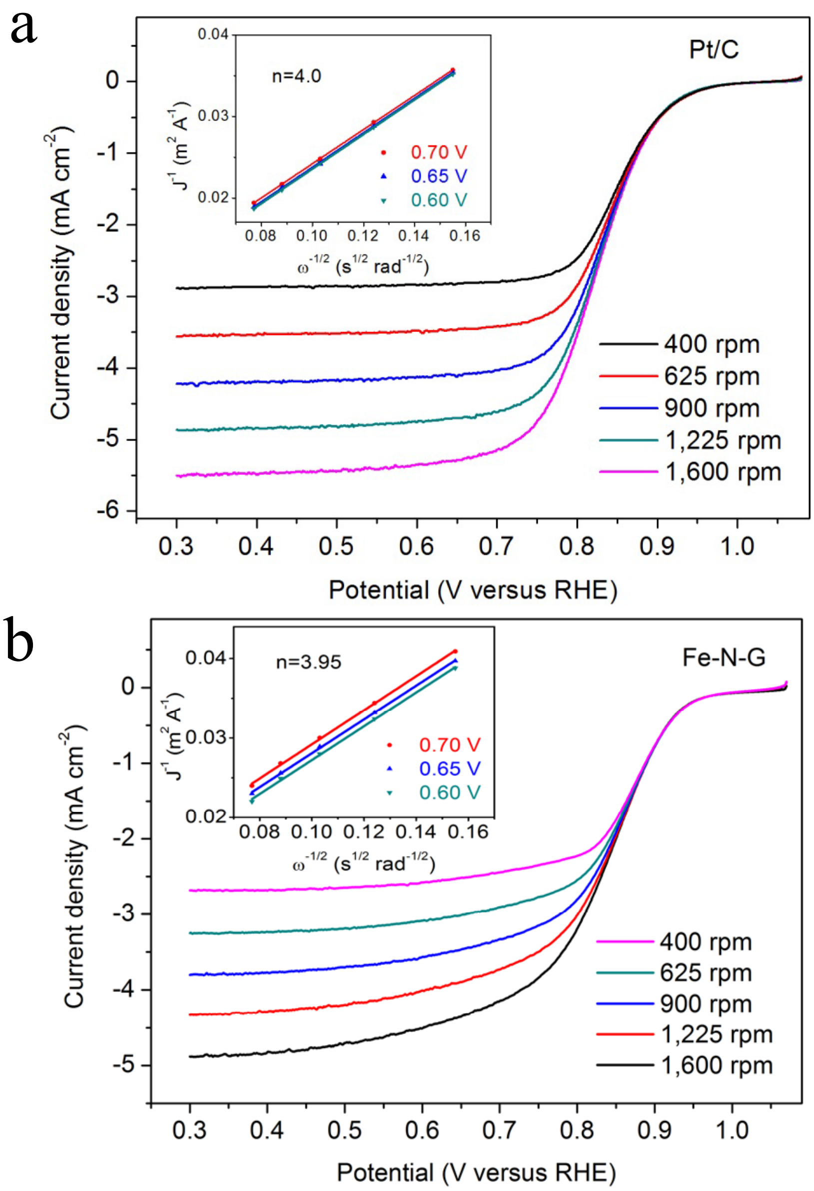

Figure S7. RDE voltammograms for (a) Pt/C (loading of 0.1 mg cm^{-2}) and (b) Fe-N-G catalysts (loading of 0.23 mg/cm^2) loaded electrodes in O_2-saturated 0.1M KOH with a potential sweep rate of 5 mV s^{-1} at different rotation rates as indicated. The insets are Koutecky–Levich plots at different potentials.

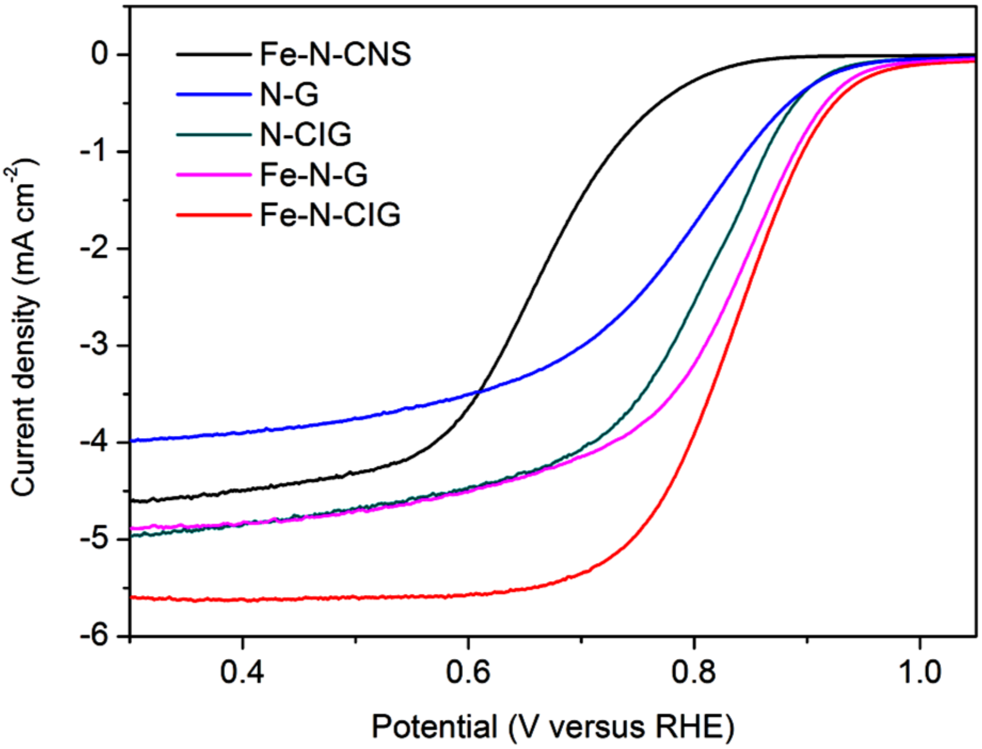

Figure S8. RDE voltammograms for Fe-N-CIG, Fe-N-CNS, N-G, N-CIG and Fe-N-G (loading of 0.23 mg/cm^2) loaded electrodes in O_2-saturated 0.1M KOH with a sweep rate of 5 mV s^{-1}at 1600 rpm.

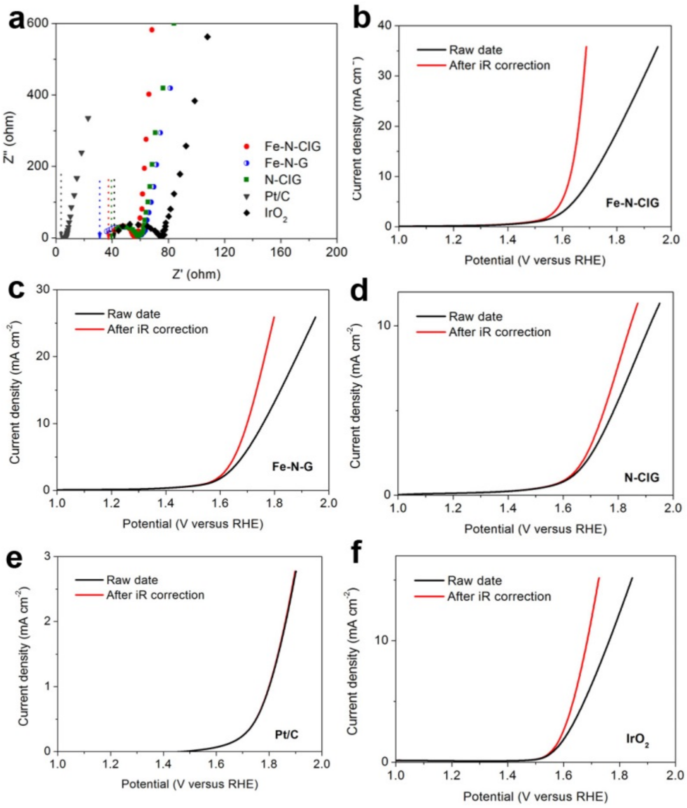

Figure S9. (a) EIS and (b-f) voltammetric curves of Fe-N-CIG (~37 Ω), Fe-N-G (~32 Ω), N-CIG (~39 Ω), Pt/C (~5 Ω), and IrO_2 (~41 Ω) loaded GC RDEs measured in 0.1 M KOH before and after *iR* corrections. High frequency limits of the EIS data were taken as the solution resistances.

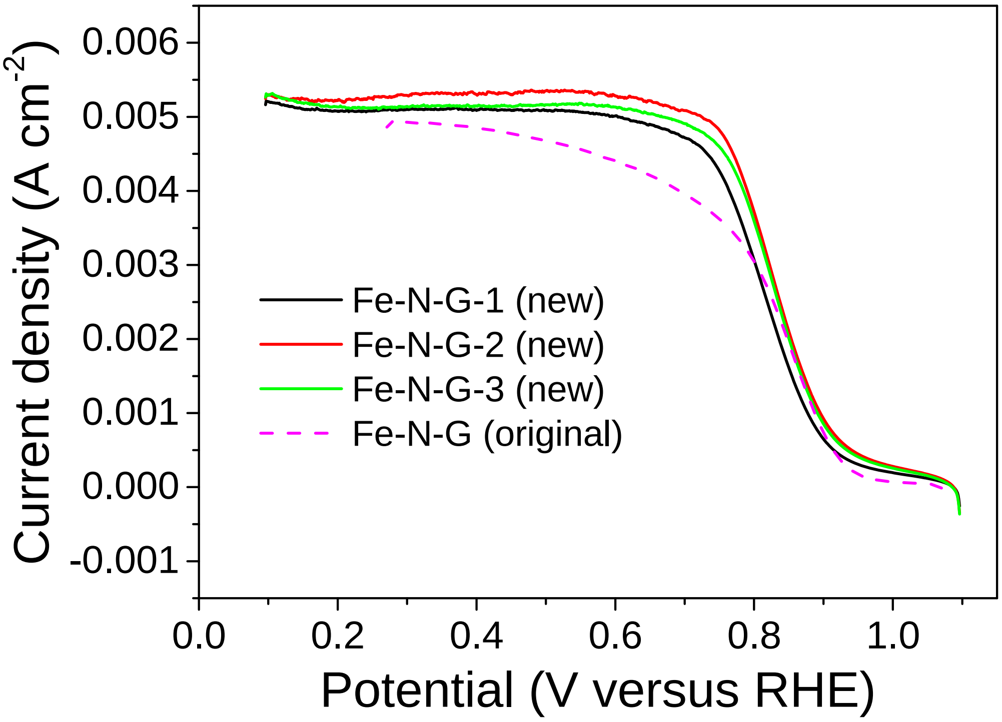

Figure S10. Steady RDE voltammograms of three occasionally obtained Fe-N-G (1, 2, and 3) samples synthesized in some batches. These catalysts exhibited enhanced ORR activities in comparison with the original Fe-N-G sample in Figure 3d. The new data could possibly indicate another mechanism to achieve an improved ORR performance of Fe-N-G, which was however not as reproducible as the Fe-N-CIG sample. Therefore, doping with conductive carbon nanospheres (Fe-N-CIG) is still an excellent and very reliable way to achieve an improved ORR activity of Fe-N-G. A systematic research is needed to investigate this new phenomenon in the future, which may lead to a new method for activity enhancement of graphene-based catalysts.